In vitro synergistic anti-prion effect of cholesterol ester modulators in combination with chlorpromazine and quinacrine

[a°]Christina D. Orrù, [a°]M. Dolores Cannas, [a]Sarah Vascellari, [a]Fabrizio Angius, [a]Pier Luigi Cocco, [a]Claudia Norfo, [b]Antonella Mandas, [a]Paolo La Colla, [a]Sandra Dessì, and [a*]Alessandra Pani

[a]Department of Biomedical Science and Technology,
[b]Department of Internal Medicine,
University of Cagliari, Italy.

°These authors contributed equally to this work.

[*]Correspondent author:
Dpt. Biomedical Science & Technology
University of Cagliari
09042-Monserrato (CA) - Italy
Phone: +39 070 675 4209
E-mail: pania@unica.it

Abstract

Background. Our studies on the role of cholesterol in prion infection/replication showed that brains and peripheral cells of sheep susceptible to or suffering from Scrapie were characterized by an altered cholesterol homeostasis compared to animals with a scrapie-resistant genotype, and that drugs influencing cholesterol esterification were endowed with selective anti-prion activity in N2a cell lines infected with the 22L and RML prion strains.

Results. In prion-infected N2a cell lines we now report increased anti-prion activity of dual-drug combinations consisting of cholesterol ester modulators associated with prion inhibitors Synergism was obtained with the cholesterol ester modulators everolimus, pioglitazone, progesterone, and verapamil associated with the anti-prion chlorpromazine, and with everolimus and pioglitazone associated with the anti-prion quinacrine. Comparative lipid analyses in prion-infected and non-infected N2a cells by colorimetric, enzymatic, and chemical means, clearly demonstrated a derangement of type and distribution of cholesterol esters, free cholesterol, and triglycerides in the infected N2a cells. Although single-drug treatments influenced lipid syntheses, only the combined-drug treatments appeared to restore a lipid profile similar to that of untreated-uninfected cells.

Conclusions. We conclude that the anti-prion synergistic effect of cholesterol ester modulators with the cholesterol metabolism interfering anti-prion drugs chlorpromazine and quinacrine may arise from the ability of combined drugs to re-establish the intracellular lipid profile of untreated-uninfected cells. Overall, these data suggest that inhibition of prion replication can be readily potentiated by combinatorial drug treatments, and that steps of cholesterol/cholesterol ester metabolism may represent suitable targets.

Abbreviations: Total lipids, (TL), neutral lipids (NL), total cholesterol (TC), cholesterol esters (CE), free cholesterol (FC), triglycerides (TG), phospholipids (PL), dextran sulphate 500,000 (DX 500), tannic acid (TA), chlorpromazine (CP), quinacrine (Q), everolimus (EVE), pioglitazone (PIO), progesterone (PG), verapamil (VP).

Introduction

Prions are unconventional infectious agents involved in fatal neurodegenerative diseases of mammals [1]. Prion replication involves conversion of cellular prion protein isoforms, named PrP^{C}, into disease-specific isoforms, designated PrP^{Sc}. Several compounds have been identified in prion-cell systems as inhibitors of the PK-resistant prion protein (PrP^{res}), and some of them have shown a protective effect in rodent prion models [2-4].

Based on the concept that combinatory strategies might prove more effective than monotherapy, Kocisko et al. [5] found, using combinations of intraventricular pentosan polysulphate (PPS) and porphyrin FeTSP, enhanced anti-scrapie effect in mice. In humans, single intraventricular PPS treatment was reported to increase the mean survival of seven prion-diseased individuals [6]. However, due to the lack of formal drug evaluation in controlled randomized studies in humans, it is not yet possible to draw any conclusion on the real effectiveness of PPS or that of several other agents tested [7]. The results of two ongoing clinical trials evaluating quinacrine in the USA (CJD quinacrine study, NCT 00183092) and in the UK (NCT 00104663, ISRCTN 06722585) are as yet unpublished.

Apart from comparative controlled studies on available drugs, efforts are being made to identify more successful therapeutic approaches, as well as novel molecular targets and inhibitors. In this context, our studies on the role of cholesterol in cell susceptibility to prion infection/replication showed that brains and peripheral cells (i.e. skin fibroblasts and blood monuclear cells) of sheep suffering from Scrapie displayed altered cholesterol homeostasis, with abnormal accumulation of cholesterol esters (CE), and altered expression of genes and gene products involved in cholesterol metabolism/trafficking [8-10]. In addition, we showed that drugs able to reduce CE content, i.e. everolimus, pioglitazone, Sandoz 58035, progesterone, and verapamil, were also able to inhibit PrP^{res} formation in persistently prion-infected N2a cells [11].

We report here enhanced anti-prion effect of selected prion inhibitors in dual-drug combinations with everolimus, pioglitazone, progesterone, and verapamil. Quinacrine and chlorpromazine were used as anti-prion agents known to prevent PrP^{res} formation in the endocytic compartment [12], whereas dextran sulphate 500,000 (DX500) and tannic acid (TA) were used as inhibitors acting on PrP^{res} formation at the plasma membrane site. Like PPS, DX500 is a sulphated polyanion which is thought to bind to PrP^{C} or PrP^{res} [13,14], whereas polyphenol tannic acid is known to stabilize plasma-membrane saturated phosphatidyl choline residues, thereby affecting PrP^{C} to PrP^{res} conversion [15].

Experimental procedure

Chemicals. Dextran sulphate sodium salt (MW 500 000), verapamil (VP) hydrochloride (98%), chlorpromazine (CP) hydrochloride, quinacrine (Q) dihydrochloride, and progesterone (PG), were purchased from Sigma-Aldrich (Italy). Tannic acid (TA) was purchased from MP Biomedicals (USA). Everolimus (EVE) was provided by Novartis (Switzerland), and pioglitazone (PIO) by Takeda (Japan). DX 500 was solubilised in OptiMEM, and stored at -20°C. EVE was solubilised in 100% ethanol and stored at +4°C. PIO was solubilised in 100% ethanol and stored at room temperature. Stock solutions of the other compounds were prepared in DMSO and stored at -20°C.

Cell lines and PrP analysis. Mouse neuroblastoma N2a cell line and sublines persistently infected with the 22L and RML strains of mouse-adapted scrapie (22L-N2a, RML-N2a), were a generous gift by Byron Caughey, NIH/NIAID Rocky Mountain Laboratories, USA. Cells were grown at 37°C, 5% CO_2, in OptiMEM supplemented with 10% FBS (Gibco, Invitrogen; Italy), 2mM L-glutamine, 50 U/ml penicillin G sodium and 50 µg/ml streptomycin sulphate

(Gibco, Invitrogen; Italy), and split every 3 to 4 days. Cell lines were stored in liquid nitrogen and working cultures were replaced every two-three months. All experiments were carried out in exponentially growing cells or sub-confluent cultures. PrP^{C} and PK-resistant PrP (PrP^{res}) were detected in cell lysates by dot blot procedure with the mouse anti-PrP antibody 6H4 (Prionics, Zurich; 1:5.000) as previously described [11].

Effect of single vs. dual drug treatments on PrP^{res} formation. Approximately 5.000 of prion-infected N2a cells in 90 µl of growth medium were added to each well of a Microtest flat-bottom 96-well plate with a low-evaporation lid (Becton Dickinson, USA). The cells were allowed to settle overnight before addition of 10 µl (10x solutions) of different concentrations of the drugs. For dual drug combinations, cell cultures were treated with 5 µl (20x solutions) of serial drug dilutions (serial ½ fractions) of each compound. Cells were either exposed to both drugs at the same time or pre-treated for 8 hours with one inhibitor before addition of the second one. DMSO in the cell medium was never higher than 0.2% (v/v). Each drug combination was tested in duplicate and each experiment was performed at least twice. After 96-hour incubation at 37°C in 5%CO_2, cells were processed for PrP^{res} detection. Autoradiography films of PrP^{res} blots were captured in TIFF format and intensity of each dot was determined through the Scion Image software (NIH). The mean value of PrP^{res} at each drug concentration and at each drug combination was expressed as a percentage of control cultures (i.e. untreated and single-drug treated cultures, respectively). EC_{50} values (50% inhibition) were determined by linear regression analysis. Duplicate cultures were drug treated as above and after 96 hours processed for evaluation of cell viability at each drug concentration/combination with the MTT method as described [11].

Type of interaction of dual drug treatments on PrP^{res} formation. The results of dual drug treatments on the generation of PrP^{res} were plotted according to the isobole method [16], a well-known procedure for the evaluation of synergism, additivity, indifference, or antagonism which requires experimental data for the agent used alone and in different dose combinations at equal-effective levels (fractions of EC_{50s}). According to this procedure, a combination is said to show zero interaction (i.e. additive) if the data points are on the straight line connecting the EC_{50} of the single agents; the points below this line correspond to synergistic interactions; those above the line indicate indifference and antagonism. To measure the degree of drugs interaction, FIC index was calculated according to the equation: $FIC = (EC50_A^{comb}/ EC50_A^{alone}) + (EC50_B^{comb}/ EC50_B^{alone})$. By this method, interactions are considered synergistic if the FIC index is <1, additive to indifferent if the FIC index is comprised between 1 and 2, and antagonistic if the FIC index is >2. The reduction in the EC_{50s} of the anti-prion drugs when they were given in combination compared to the EC_{50s} when given alone, were compared through a paired rank test, a non parametric test for comparison between two related samples. A p value < 0.05 was considered significant.

Evaluation of drug efflux activity. Drug efflux activity of P-gp protein was determined by measuring intracellular accumulation of radioactive vinblastine as previously described [17]. In brief, 22L-N2a cells were seeded at $1x10^4$ cells/ml in growth medium (OptiMEM supplemented with 10% FCS, 100 units/ml penicillin, 100 µg/ml streptomycin) in a Microtest flat-bottom 24-well plate with a low-evaporation lid (Becton Dickinson, USA). Cultures were allowed to settle overnight and then further incubated in the absence and in the presence of different concentrations of the cholesterol inhibitors. After 96 hours of incubation, cell cultures were washed twice with PBS and re-incubated at 37 °C in ½ final volume of fresh growth medium containing or not the drugs. One hour later, cells were re-fed with equal volume of identical pre-warmed medium supplemented with 0.1 µCi/ml [G-^{3}H]vinblastine sulfate (15.5 Ci/millomole; Amersham Life Sci.). After 1-hour pulse, cell monolayers were rapidly washed 3 times with ice-

cold PBS, solubilized in 0.1N NaOH, and analyzed for protein and [G-^{3}H]-vinblastine content in a Beckman β-Counter. The amount of intracellular [G-^{3}H]-vinblastine is reported as CPM per μg of total cellular protein, as determined by the bicinchoninic acid (BCA) protein assay (Sigma-Aldrich) [11]. Each determination was performed in triplicate.

Intracellular lipid staining. To visualize intracellular lipids, N2a and 22L-N2a cells were seeded at 1x10^4/ml in growth medium in Microtest flat-bottom 24-well plates (Becton Dickinson, USA). After overnight settlement, 22L-N2a cultures were drug-treated under conditions used for evaluation of anti-PrP^{res} activity. Each drug and drug combination was tested in triplicate. After 96-hour incubation, untreated and drug treated cultures were washed with PBS, fixed by soaking in 10% formalin and then stained with Oil red-O (ORO) (Sigma), Nile red (9-diethylamino-5H-benzo[α]phenoxazine-5-one, Fluka, Buchs, SG, Switzerland) and filipin (Sigma). ORO is a lipid-soluble dye which stains NL (i.e. CE and TG), but not FC. ORO staining was performed in 60% isopropyl alcohol, followed by Mayer's hematoxylin counterstaining for nuclei [11]. After staining, cells were imaged using a Leitz inverted-phase microscope fitted with a digital camera. NL appear as bright red spots in the cell cytoplasm. At least two different fields per sample were imaged and analyzed. Red ORO intensity was quantified by NIH Image J software utilizing four different selected regions of interest (ROIs), and values arbitrarily expressed as mean pixels± SE/cm^2 of triplicate wells. Nile red is a fluorescent dye that stains differentially polar lipids (i.e. phospholipids, PL) and NL (i.e. CE and TG) [18]. PL show a prevalent red emission, while NL show both red and green emission. Red emission was observed with 540±12.5 excitation and 590 LP emission filters. Green emission was observed with 460±25 excitation and 535±20 emission filters. Filipin is a fluorescent dye which stains only FC (blue emission). Filipin was observed with 360±20 excitation and 460±25 emission filters. Filipin and Nile red emissions were completely separated by the above indicated filters, so the two fluorochromes could be used in combination on the same cells [19]. Quantitative image analysis was performed with the ImagePro Plus package (Media Cybernetics, Silver Springs, MD).

Cellular lipid content, synthesis, and efflux. For determinations of the different lipid subclasses in N2a and 22L-N2a cells, TL were extracted with cold acetone from a total of 30x10^6 of each cell line collected from sub-confluent flasks. Extracted lipids were split into two equal aliquots and air dried: one aliquot was used to determine TC by the cholesterol oxidase method (Sclavo Diagnostics, Siena, Italy); the other aliquot, after drying, was resuspended in 100 μl of chloroform and analysed for lipid subclasses by thin layer chromatography (TLC) on kiesegel plates using a solvent system containing n-heptane/isopropyl ether/formic acid (60:40:2 v/v/v). Separated bands were identified as FC, CE, and TG by comparison with reference standards run simultaneously side-by-side and visualized under iodine vapors. Bands were excised and their masses determined by the cholesterol oxidase (for FC and CE) and peroxidase (for TG) assay methods (Sclavo Diagnostics, Siena, Italy). To determine the effect of drugs and drug combinations on lipid synthesis and efflux, N2a and 22L-N2a cells were seeded at 1x10^4/ml in growth medium in Microtest flat-bottom 24-well plates (Becton Dickinson, USA). After overnight settlement, 22L-N2a cultures were drug-treated and incubated under the condition used for evaluation of anti-PrP^{res} activity. Each drug and drug combination was tested in triplicate. Six hours before harvesting, 5 μCi/ml sodium ^{14}C-acetate (DuPont, NEN; specific radioactivity 50 mCi/mmol) were added to each well. At the end of labelling, TL in the cell monolayers and in the growth media were extracted with cold acetone and lipid subclasses separated by TLC as described above. The incorporation of ^{14}C-acetate into lipid sub fractions was measured in a Liquid

Scintillation Counter. Efflux of ^{14}C-TL was expressed as the percentage of the radioactivity recovered in medium/total radioactivity (cells + medium).

Statistical analysis. Unless otherwise indicated, data are reported as mean ± standard error (SE). Statistical calculations were performed using the statistical analysis software Origin 8.0 version (Microcal, Inc, Northampton, MA, USA). Data analysis was done using the Student t-test. A value of $p<0.05$ was considered to be statistically significant.

Results

Anti-PrP^{res} activity of prion inhibitors in combination with CE modulators.

The inhibitory effect of single vs. dual-drug treatments on PrP^{res} generation was evaluated in 22L-infected cells by dot blot procedure [20], a method equally reliable but more suitable than Western blot-based assay for comparative studies of multiple drugs. 22L-N2a cell cultures were exposed to fractions of the EC_{50} (serial ½ drug dilutions) of each compound, alone and in association. Dual-drug treatments were either performed at the same time or in sequential order: 8 hrs treatment with one drug before adding the second drug. Type and degree of drug interactions were analyzed by both isobole and FIC index methods [16]. The effect of combined treatments ranged from synergism to indifference, depending on the prion inhibitor considered, drug concentration, and the temporal sequence of drug addition. Simultaneous treatments, as well as sequential combination with prion inhibitors which preceded CE modulators, always resulted in an additive or indifferent type of interaction (not shown).Sequential combinations comprising any CE modulator followed by DX500 or TA also resulted in an additive or indifferent type of interaction. Isoboles and FIC indices of combinations comprising EVE and PG followed by DX500 and TA are shown in Fig.1A. By contrast, a marked enhancement of the anti-prion effect was obtained when cells were treated with any CE modulator followed by CP. Pre-treatments with EVE, PIO, PG, or VP, resulted in anti-prion effects in the range of synergism, as indicated by either FIC values (0.21-0.73) or data points in isoboles (Fig.2A). Significant reduction of CP EC_{50} (10 to 1.8μM [p <0.01]), EVE (1 to 0.1μM [p <0.01]), PIO (40 to 5μM [p <0.05]), PG (35 to 5μM [p <0.05]), and VP (10 to 2.5μM [p<0.05]) was observed. Sequential combinations of CE modulators followed by Q resulted in different drug interactions, depending on the dose and type of CE modulator. Pre-treatments with low doses of EVE, PIO, and PG resulted in synergistic interactions (FIC values: 0.18-0.25, EVE; 0.29-0.5, PIO; 0.70-0.71, PG), while higher doses resulted in additive effects. VP showed additive interaction at any concentration (FICs 0.95-1.13) (Fig.3A). Significant reduction of Q EC_{50} (1 to 0.1μM [p <0.01]), EVE (1 to 0.08μM [p <0.01]), and PIO (40 to 5μM [p <0.05]) was observed. Representative dot blots after single and dual-drug combination treatments comprising EVE, DX500, CP, and Q are shown (Fig.1-3B). Notably, similar drug interactions against PrP^{res} formation were also obtained in N2a cells infected with the RML prion strain (data not shown). Anti-prion effects were not due to cytotoxicity, as neither single nor dual-drug treatments affected cell viability and proliferation at active concentrations (Table 1).

Effect of CE modulators on P-gp drug efflux activity.

In multidrug-resistant cell lines, PG and VP are known chemo-sensitizers of unrelated cytotoxic agents via the inhibition of membrane drug-efflux P-gp protein [21, refs therein]. To investigate whether synergism was due to increased CP and Q cell retention, the overall drug-efflux potential of 22L-N2a cells was investigated. Cells were exposed to the CE modulators for either 1 hour (i.e. standard procedure for measuring drug-efflux P-gp activity) or 96 hours (i.e. our test condition to evaluate anti-prion activity), and then pulse-labelled with ^{3}H-

vinblastine, a known P-gp substrate [17,21]. VP and PG, at concentrations close to their EC_{50s} (i.e. 10μM and 35μM, respectively), increased intracellular vinblastine content with respect to untreated cultures (Table 2). VP resulted a better P-gp inhibitor than PG and determined higher vinblastine influx after both short (1 hr) and prolonged (96 hrs) exposure to the drug. However, treatments with concentrations (i.e. 7.5μM and 2.5μM, respectively) closer to synergistic ones, had no effect on vinblastine retention. EVE showed negligible anti-P-gp activity following treatments with 1 μM and 0.5 μM, and had no effect at a dose (0.05 μM) higher than that showing the strongest anti-prion synergism in combination with both CP and Q. Intriguingly, a high dose of PIO (40 μM), while not affecting vinblastine influx after short treatment, determined a marked retention of labelled vinblastine after prolonged treatment.

Effect of single vs. dual-drug combinations on intracellular lipids.

Given that it was unlikely that observed synergisms were due to intracellular retention of anti-prion drugs, we investigated whether the combined drugs interacted at the level of lipid metabolism. The effect on intracellular lipids of a drug combination with marked anti-PrP^{res} synergism, such as EVE (0.02 μM) and CP (2 μM), was initially determined by staining cells with dyes with affinity for different lipids (ORO, NL; Nile red, NL and PL; filipin, FC). As expected [11], ORO staining revealed significantly higher NL in the 22L-N2a compared to uninfected N2a cells (Fig.4A and B). However, both single and combined drug treatments markedly reduced red ORO intensity in the 22L-infected cell line. More detailed information was obtained with Nile red, a fluorescent hydrophobic probe that, being based on the different sensitivity of red and green emissions to low- and high-hydrophobic lipids, respectively, allowed us to distinguish neutral from polar (i.e. membrane PL) lipids. Combined staining with Nile red and filipin, a fluorescent sterol binding agent, allowed us to also co-localize FC (blue emission). With respect to uninfected cells, 22L-infected cultures showed an increase in both polar and neutral lipids, as well as in FC (Fig. 5A and B). In agreement with ORO data, 22L-N2a cells showed a higher green emission signal - indicative of higher NL content. However, in the cytoplasm most of the green Nile-red staining was spread, rather than being localized in large lipid droplets. 22L-N2a cells showed also a more intense filipin fluorescence - indicative of a higher FC content, some of which was spread in the cytoplasm. Single treatment of infected cultures with EVE determined a marked reduction of all forms of intracellular lipids, whereas treatment with CP had a lower, although significant, effect on both PL and CE, but no significant effect on FC. Interestingly, combined EVE and CP treatments of infected cells appeared to re-establish the intracellular lipid profile of untreated-uninfected cells.

Lipid content in N2a vs. 22L-N2a by TLC.

The above data clearly indicate that 22L-infected cells displayed higher NL compared to uninfected cells. However, there was a marked difference in dye intensity values between ORO and Nile red staining: compared to N2a, 22L-N2a cells showed over 5-fold-higher ORO stain and only approximately 1.5-fold-higher green Nile-red fluorescence. This discrepancy led us to more accurately determine the lipid content in N2a and 22L-N2a cell extracts. As seen in Figure 6 (A and B), the cholesterol oxidase assay revealed a TC content 1.7-fold higher in infected cells. TLC separation of lipid subclasses showed that 22L-N2a cells had higher levels of both FC (1.6-fold) and CE (5.5-fold) than N2a cultures, with 3.1 and 10.3 FC/CE ratios, respectively. Extracts of infected cells had also 1.9-fold higher levels of TG. Lipid determination by enzymatic and chemical means confirmed, even though not in a

stoichiometric manner, that infected cells display a higher level of all lipid sub-fractions, and additionally identified CE as the most altered of all lipid subclasses.

Effect of single vs. dual-drug combinations on lipid synthesis and efflux in 22L-N2a.

To draw more consistent conclusions regarding the effects of drugs and drug combinations on cellular lipid homeostasis, we compared lipid neosynthesis (FC, CE, TG) and lipid efflux (mainly FC) in N2a vs. 22L-infected N2a cells, either untreated or treated with single and dual-drug combinations of EVE (0.02 μM), CP (2 μM), and Q (0.2 μM). Once again, ^{14}C-acetate incorporated into TL was higher in the 22L-N2a than in N2a cells (Fig.7A). In spite of a slight increase in TL efflux in the 22L-infected cultures, the percentage of TL efflux did not significantly differ between the two cell lines. TLC separation of lipid subclasses showed that the higher lipid syntheses in the 22L-N2a cells was due to increased neosynthesis of FC (1.5-fold), CE (2-fold), and TG (1.6-fold) (Fig.7B). In 22L-N2a cells, both single and combined drug treatments greatly affected all lipid syntheses. However, single-drug treatments differently affected the synthesis of each individual lipid type, whereas combined drugs appeared to restore all lipid syntheses to the levels observed in untreated-uninfected cells (Fig.7A and B).

Discussion

Drugs targeting steps of cholesterol metabolism/esterification were found by us to enhance the anti-prion activity of chlorpromazine and quinacrine, by reducing their EC_{50s} up to 10-fold. Synergistic drug interactions were obtained in sequential combination of chlorpromazine or quinacrine with i) everolimus (an immunosuppressant agent that inhibits cholesterol esterification by an as yet unknown mechanism) [22,23]; ii) pioglitazone (an anti-diabetic drug that induces cell redistribution of free fatty acids) [24]; iii) verapamil (a calcium-blocking drug that inhibits cholesterol trafficking from the plasma membrane to the endoplasmic reticulum) [21, refs therein]; and iv) progesterone (a sterol hormone that affects cholesterol trafficking from both the plasma membrane and lysosomes) [25,26]. Chlorpromazine and quinacrine are known to inhibit prion *in vitro* and to some extent also *in vivo* [2,27]. Although the exact mechanism(s) remains to be established, these drugs have been involved in: i) competitive inhibition of endogenous sulfated glycosaminoglycans (GAGs)-PrP interaction, essential for PrP^{res} formation or stabilization in the endosomes; ii) unfolding of PrP^{res} by drug-induced endosome/lysosome accumulation of chaperone-like factor(s); iii) destabilization of PrP^{res} by alteration of lysosomal pH [12]. Recent evidence, however, not formally excluding the above mechanisms, indicates that quinacrine and chlorpromazine might exert anti-prion effect by additional mechanisms that involve interference with intracellular cholesterol. Quinacrine has been reported to determine destabilization of cholesterol-rich membrane domains (DRMs or rafts) [28]. Worthy of note, these Authors also described a synergistic anti-prion effect of quinacrine in combination with simvastatin, a known inhibitor of cholesterol biosynthesis, and the anti-prion activity of progesterone. As for chlorpromazine, a study on the role of cellular cholesterol in the pathogenesis of schizophrenia, indicated that drug-induced transcriptional activation of cholesterol biosynthesis could represent a novel mechanism of action for some antipsychotic drugs, chlorpromazine being one of the most potent [29]. Hence, observed anti-PrP^{res} synergistic effects may arise from the interaction of drugs affecting cellular cholesterol metabolism at different levels. Although suffering from quantitative discrepancies, probably due to the different detection sensitivities of the various techniques used, the results obtained in the 22L-infected N2a cells by ORO, Nile red, and filipin staining, as well as by enzymatic

and chemical methods, clearly indicate a derangement of type and distribution of intracellular lipids, possibly at the expense of plasma membrane functional integrity. Compared to N2a, 22L-infected N2a cells displayed significant higher content and neosynthesis of FC, CE, and TG, coupled with no variation in cholesterol efflux; the CE sub-fraction appearing the most altered. These results are in agreement with a number of previous studies on mouse brains during the course of prion infection, showing altered cholesterol metabolism/esterification with an over-expression of the enzyme responsible for intracellular cholesterol esterification, ACAT1 (*soat1*) [30, refs therein]. Altered cholesterol homeostasis may affect functional integrity of membrane lipid domains leading to altered clustering process of raft-resident proteins and to increased conversion of PrP^{C} into the misfolded isoform [31]. The ability of combined treatments of everolimus and chloropromazine, or everolimus and quinacrine, to restore intracellular content and distribution of PL, NL, and FC similar to uninfected-untreated N2a cells supports this hypothesis and may account for the enhanced anti-prion effect of these drug combinations. On the other hand, a mechanism involving inhibition of the drug-efflux pump P-gp seems unlikely. Firstly, most synergistic effects against PrP^{res} were obtained with P-gp inhibitors (progesterone and verapamil) at concentrations 4/5-fold lower than those required to increase vinblastine influx. Secondly, everolimus, at the highest concentration tested (i.e. 1 μM) increased vinblastine retention by only 10%. Worthy of note, a recent study by Bate et al. reported a higher toxicity of some ACAT inhibitors (i.e. TMP-153, FR179254 and YIC-C8-434) in prion-infected ScGT1 and ScN2a cell lines vs. uninfected cells [32]. However, none of the CE modulators used in the present study affected the viability of 22L-infected and uninfected N2a cells, neither in single nor in combinatory drug experiments.

Taken together these results indicate that inhibition of prion replication can be readily potentiated by combinatorial drug treatments and that steps of cholesterol/cholesterol ester metabolism may represent suitable targets. Indeed, in prion-infected N2a cells, that clearly displayed altered lipid homeostasis, the combined treatments with CE modulators associated with cholesterol metabolism interfering anti-prion drugs, appear to re-establish the intracellular lipid profile of untreated-uninfected cells.

Some findings in this study have been the subject of patent applications PCT/IT2007/000109 (Methods for the therapy of proliferative and/or conformational diseases) and PCT/IT2007/000110 (Methods for the diagnosis of proliferative and/or conformational diseases), inventors S. Dessì, P. La Colla, and A. Pani.

Acknowledgements

This work was in part supported by a grant from Regione Autonoma Sardegna. The Authors are indebted with Byron Caughey (NIH/NIAID Rocky Mountain Laboratories, USA) for kindly providing mouse neuroblastoma cell lines. We also thank Mr. Edward Steeden for editing the English.

References

[1] Prusiner S.B. Prions. Proc. Natl. Acad. Sci., USA 1998, 95, 13363-13383.

[2] Trevitt C.R., Collinge J. A systematic review of prion therapeutics in experimental models. Brain 2006, 129, 2241-65.

[3] Doh-ura K., Ishikawa K., Murakami-Kubo I., Sasaki K., Mohri S., Race R., Iwaki T. Treatment of transmissible spongiform encephalopathy by intraventricular drug infusion in animal models. J. Virol., 2004, 78, 4999-5006.

[4] Love R. Old drugs to treat new variant Creutzfeldt-Jakob disease. Lancet 2001, 358, 563-574.
[5] Kocisko D., Caughey B., Morrey J.D., and Race R.E. Enhanced antiscrapie effect using combination drug treatment. Antimicrob. Agents Chemother., 2006, 50, 3447-3449.
[6] Bone I., Belton L., Walker A.S., Darbyshire J. Intraventricular pentosan polysulphate in human prion diseases: an observational study in the UK. Eur. J. Neurol. 2008, 15, 458-464.
[7] Stewart L.A., Rydzewska L.H.M., Keogh G.F., Knight R.S.G. Systematic review of therapeutic interventions in human prion disease. Neurology 2008, 70, 1272-1281.
[8] Pani A., Abete C., Norfo C., Mulas C., Putzolu M., Laconi S., Cannas M.D., Orrù C.D., La Colla P., Dessì S. Cholesterol metabolism in brain and skin fibroblasts from Sarda breed sheep with scrapie resistant or susceptible genotype. Am. J. Infect. Dis. 2007, 3, 143-150.
[9] Pani A., Abete C., Norfo C., Mulas C., Putzolu M., Laconi S., Orrù C.D., Cannas M.D., Vascellari S., La Colla P., Dessì S. Accumulation of CE in ex vivo lymphocytes from scrapie-susceptible sheep and in scrapie-infected mouse neuroblastoma cell lines. Am. J. Infect. Dis. 2007, 3, 165-168.
[10] Pani A., Putzolu M., Mulas C., Orrù C.D., Abete C., Norfo C., Cannas M.D., Laconi S., La Colla P. and Dessì S. ACAT1, Cav-1, and PrP Expression In Brains And Skin Fibroblasts From Sarda Breed Sheep With Scrapie-Resistant And Scrapie-Susceptible Genotype. Available from Nat Precedings, 2007. http://precedings.nature.com/documents/1211/version/1
[11] Pani A., Norfo C., Abete C., Mulas C., Putzolu M., Laconi S., Orrù C.D., Cannas M.D., Vascellari S., La Colla P., Dessì S. Anti-prion activity of cholesterol esterification modulators: a comparative study in ex vivo sheep fibroblasts and lymphocytes and in mouse neuroblastoma cell lines. Antimicrob. Agents Chemother. 2007, 51, 4141-4147.
[12] Doh-ura K., Iwaki T., Caughey B. Lysosomotropic Agents and Cysteine Protease Inhibitors Inhibit Scrapie-Associated Prion Protein Accumulation. J. Virol. 2000, 74, 4894-4897.
[13] Caughey B., Raymond G.J. Sulfated polyanion inhibition of scrapie-associated PrP accumulation in cultured cells. J. Virol. 1993, 67, 643-50.
[14] Caughey B., Brown K., Raymond G.J., Katzenstein G.E., Thresher W. Binding of the protease-sensitive form of PrP (prion protein) to sulfated glycosaminoglycan and congo red. J. Virol., 1994, 68, 2135-2141.
[15] Kocisko D.A., Engel A.L., Harbuck K., Arnold K.M., Olsen E.A., Raymond L.D., Vilette D., Caughey B. Comparison of protease-resistant prion protein inhibitors in cell cultures infected with two strains of mouse and sheep scrapie. Neurosci. Lett., 2005, 388, 106-111.
[16] Suhnel J. Evaluation of synergism or antagonism for the combined action of antiviral agents. Antiv. Res., 1990, 13, 23-40.
[17] Pani A., Batetta B., Putzolu M., Sanna F., Spano O., Piras S., Mulas M.F., Bonatesta R.R., Amat di S.Filippo C., Vargiu L., Marceddu T., Sanna L., La Colla P., Dessì S. MDR1, cholesterol esterification and cell growth: a comparative study in normal and multidrug-resistant KB cell lines. Cell. Mol. Life Sci., 2000, 57, 1094-1102.
[18] Greenspan P., Fowler S.D. Spectrofluorometric studies of the lipid probe, Nile red. J. Lipid Res., 1985, 26, 781-789.
[19]. Diaz G., Batetta B., Sanna F., Uda S., Reali C., Angius F., Melis M., Falchi A.M. Lipid droplet changes in proliferating and quiescent 3T3 fibroblasts. Histochem. Cell Biol., 2008, 129, 611-621.

[20] Kocisko D.A., Baron G.S., Rubenstein R., Chen J., Kuizon S., Caughey B. New inhibitors of scrapie-associated prion protein formation in a library of 2000 drugs and natural products. J. Virol. 2003, 77, 10288-10296.
[21] Pani A. and Dessì S. Cell Growth and Cholesterol Esters. Eds Pani and Dessì. New York: Landes Bioscence & Kluwer Academic Press Publishers, 2004.
[22] Batetta B., Mulas M.F., Sanna F., Putzolu M., Bonatesta R.R., Casperi-Campani A., Roncuzzi L., Baiocchi D., Dessì S. Role of cholesterol ester pathway in the control of cell cycle in human aortic smooth muscle cells. FASEB J., 2003, 17, 746-748.
[23] Varghese Z., Fernando R., Moorhead J.F., Powis S.H., Ruan X.Z. Effects of sirolimus on mesangial cell cholesterol homeostasis: a novel mechanism for its action against lipid-mediated injury in renal allografts. Am. J. Physiol. Renal Physiol. 2005, 289, 43-48.
[24] Freeman D.A., Romero A. Effects of troglitazone on intracellular cholesterol distribution and cholesterol-dependent cell functions in MA-10 Leydig tumor cells. Biochem. Pharmacol. 2003, 66, 307-313.
[25] Debry P., Nash E.A., Neklason D.W., Metherall J.E. Role of multidrug resistance P-glycoproteins in cholesterol esterification. J. Biol. Chem., 1997, 272, 1026-1031.
[26] Butler J.D., Banchette-Mackie J., Golden E., O'Neill R.R., Carstea G., Roff C.F., Patterson M.C., Patel S., Comly M.E., Cooney A., Vanier M.T., Brady R.O., Pentchev P.G. Progesterone blocks cholesterol translocation from lysosomes. J. Biol. Chem., 1992, 267, 23797-23805.
[27] Barret A., Tagliavini F., Forloni G., Bate C., Salmona M., Colombo L., De Luigi A., Limido L., Suardi S., Rossi G., Auvrè F., Adjou K.T., Salès N., Williams A., Lasmèzas C., Deslys J.P. Evaluation of quinacrine treatment for prion diseases. J. Virol. 2003, 77, 8462-8469.
[28] Klingenstein R., Lober S., Kujala P., Godsave S., Leliveld S.R., Gmeiner P., Peters P.J., Korth C. Tricyclic antidepressants, quinacrine and a novel, synthetic chimera thereof clear prions by destabilizing detergent-resistant membrane compartments. J. Neurochem., 2006, 98, 748-59.
[29] FernØ J., Skrede S., O Vik-Mo A., Havic B., Steen V.D. Drug-induced activation of SREBP-controlled lipogenic gene expression in CNS-related cell lines: marked differences between various antipsychotic drugs. BMC Neuroscience, 2006, 7, 69-80.
[30] Kumar R., McClain D., Young R., Carlson G.A. Cholesterol transporter ATP-binding cassette A1 (ABCA1) is elevated in prion disease and affects PrPC and PrPSc concentrations in cultured cells. J. Gen. Virol. 2008, 89, 1525-32.
[31] Taylor D.R. and Hooper N.M. Role of lipid rafts in the processing of the pathogenic prion and Alzheimer's amyloid-β proteins. Sem. Cell. Develop. Biol., 2007, 18. 638-648.
[32] Bate C., Tayebi M., Williams A. Cholesterol esterification reduces the neurotoxicity of prions. Neuropharmacol. 2008, 54, 1247-1253.

Table 1. Cytotoxicity of single vs. dual drug treatments in 22L-infected N2a cells.

		DX 500 μM				CC_{50}	CP μM			CC_{50}	Q μM				CC_{50}
		1x 10^{-15}	5 x10^{-16}	2.4 x10^{-16}	1.2 x10^{-16}	1 x10^{-16}	10	5	2.5	1.25	98±11	1	0.5	0.25	0.12	4.5±1.3
	CC_{50}	Mean cell viability (% of controls)														
EVE μM	1.2±.2															
0.5		100±2	100±2	100±2	100±2		98±3	100±2	100±2	100±2		93±2	98±1	100±2	100±2	
0.25		100±2	100±2	100±2	100±2		100±2	100±2	100±2	100±2		94±1	100±2	100±2	100±2	
0.12		100±2	100±2	100±2	100±2		100±2	100±2	100±2	100±2		100±2	100±2	100±2	100±2	
0.06		100±2	100±2	100±2	100±2		100±2	100±2	100±2	100±2		100±2	100±2	100±2	100±2	
		Mean cell viability (% of controls)														
PIO μM	53±4.1															
40		75±2	74±1	75±3	73±1		96±3	92±3	92±3	94±1		79±4	80±3	78±3	79±2	
20		84±2	83±3	80±2	83±1		100±2	100±2	100±2	100±2		90±3	94±2	95±2	99±1	
10		100±2	100±2	100±2	100±2		100±2	100±2	100±2	100±2		94±	100±2	100±2	100±2	
5		100±2	100±2	100±2	100±2		100±2	100±2	100±2	100±2		100±2	100±2	100±2	100±2	
		Mean cell viability (% of controls)														
VP μM	97±8.7															
10		100±2	100±2	100±2	100±2		100±2	100±2	100±2	100±2		89±3	100±2	100±2	100±2	
5		100±2	100±2	100±2	100±2		100±2	100±2	100±2	100±2		93±3	100±2	100±2	100±2	
2.5		100±2	100±2	100±2	100±2		100±2	100±2	100±2	100±2		93±2	100±2	100±2	100±2	
1.25		100±2	100±2	100±2	100±2		100±2	100±2	100±2	100±2		100±2	100±2	100±2	100±2	
		Mean cell viability (% of controls)														
PG μM	135±8.8															
30		100±2	100±2	100±2	100±2		69±5	82±2	89±1	99±3		90±3	95±1	100±2	100±2	
15		100±2	100±2	100±2	100±2		90±3	98±1	100±2	100±2		93±2	99±1	100±2	100±2	
7.5		100±2	100±2	100±2	100±2		97±3	100±2	100±2	100±2		92±1	100±2	100±2	100±2	
3.75		100±2	100±2	100±2	100±2		100±2	100±2	100±2	100±2		100±2	100±2	100±2	100±2	

Values represent the mean ±SD of duplicate samples from three independent experiments.

Table 2. MDR1/P-gp drug efflux activity in 22L-infected N2a cell lines.

		[^{3}H]-VBL CPM/µg protein ± SD	
Drug	[µM]	1 hour	96 hours
No drug	-	28.11±3.3	36.30±2.2
Progesterone	35	37.28±3.1	41.85±2.2
	15	32.18±2.5	36.10±1.6
	7.5	28.43±2.9	36.32±2.5
Verapamil	10	60.68±4.2	63.79±3.9
	5	45.77±3.3	39.21±3.6
	2.5	28.34±1.7	36.06±1.0
Everolimus	1	30.59±1.9	35.85±2.4
	0.5	28.32±2.1	33.63±2.2
	0.05	28.04±2.8	34.87± 1.7
Pioglitazone	40	30.39± 2.2	50.73±3.8
	20	28.65±3.1	37.33±3.3
	10	28.88±2.0	36.73±1.1

Values represent the mean ±SD of triplicate determinations from three independent experiments.

Figure 1.

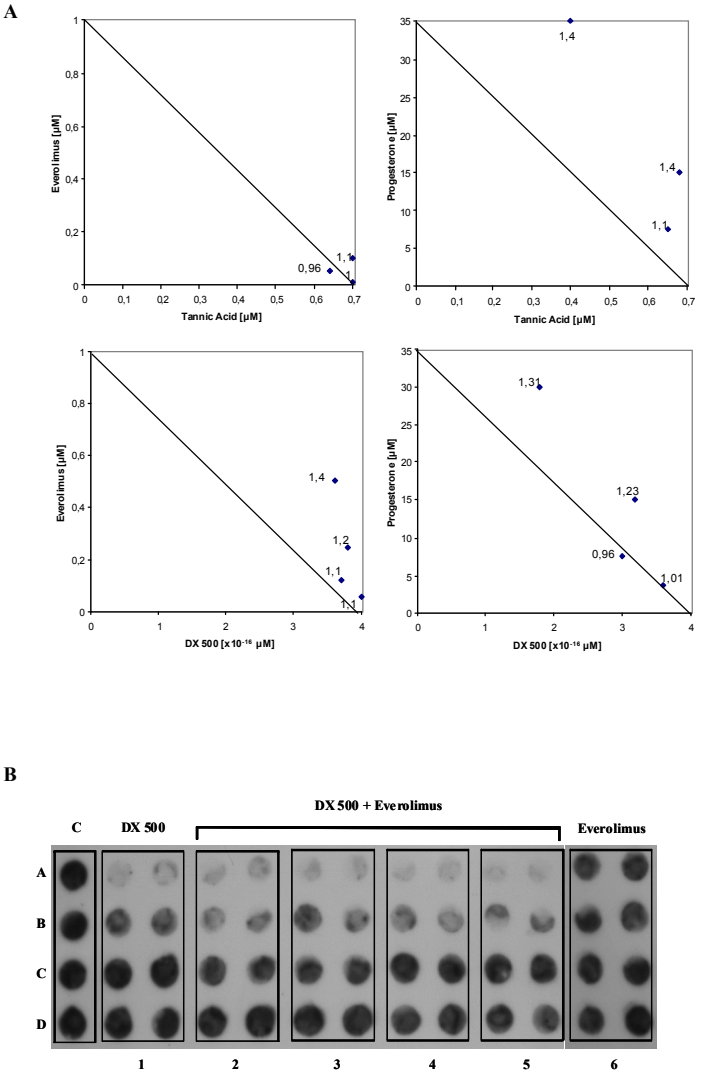

Figure 1. Anti-prion activity of tannic acid and DX500 in combination with everolimus and progesterone. Prion-infected 22L-N2a cells were pre-treated for 8 hours with different concentrations of everolimus or progesterone prior to the addition of different concentrations of tannic acid or DX500. After 96 hours, cells were lysed and processed for detection of PrP^{res} by dot blot with mouse monoclonal 6H4 antibody (Prionics). A) Isoboles and FIC indices of drug combinations. B) Representative dot blots of anti-prion effects of everolimus (EVE) and DX500, alone and in combination. Controls (C A-D). DX500 alone: 0.5 µg/ml (A1); 0.25 µg/ml (B1), 0.125 µg/ml (C1); 0.06 µg/ml (D1). EVE alone: 0.5 µM (A6); 0.25 µM (B6); 0.125 µM (C6), 0.06 µM (D6). EVE 0.5 µM (A-D2) with DX500 0.5 µg/ml (A2); DX5000.25 µg/ml (B2), DX500 0.125 µg/ml (C2); DX500 0.06 µg/ml (D2). EVE 0.25 µM (A-D3) with DX500 0.5 µg/ml (A3); DX5000.25 µg/ml (B3), DX500 0.125 µg/ml (C3); DX500 0.06 µg/ml (D3). EVE 0.125 µM (A-D4) with DX500 0.5 µg/ml (A4); DX500 0.25 µg/ml (B4), DX500 0.125 µg/ml (C4); DX500 0.06 µg/ml (D4). EVE 0.06 µM (A-D5) with DX500 0.5 µg/ml (A5); DX5000.25 µg/ml (B5), DX500 0.125 µg/ml (C5); DX500 0.06 µg/ml (D5).

Figure 2.

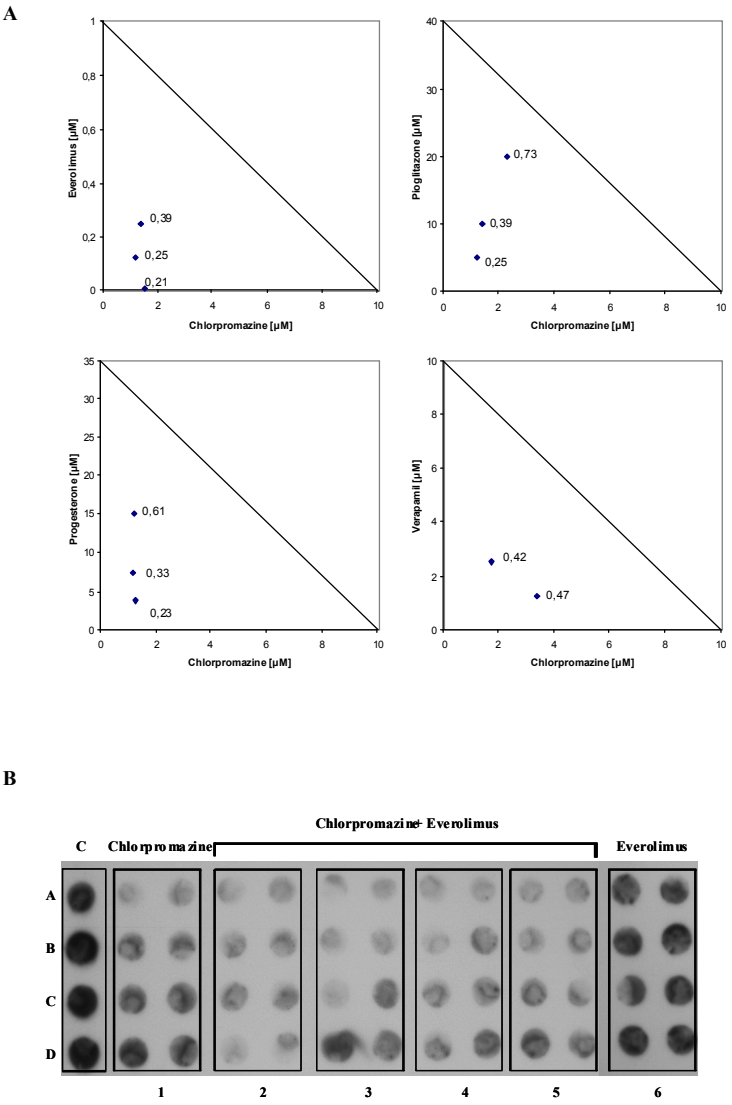

Figure 2. Anti-prion activity of chlorpromazine in combinations with everolimus, pioglitazone, progesterone, and verapamil. Prion-infected 22L-N2a cells were treated for 8 hours with different concentrations of everolimus, pioglitazone, progesterone, and verapamil prior to the addition of different concentrations of chlorpromazine. After 96 hours cells were lysed and processed for detection of PrP^{res} by dot blot with mouse monoclonal 6H4 (Prionics). A) Isoboles and FIC indices of combinations. B) A representative dot blot of the anti-prion effect of everolimus (EVE) and chlorpromazine (CP), alone and in combination. Controls (C A-D). CP alone: 10 µM (A1); 5 µM (B1); 2.5 µM (C1) and 1.25 µM (D1). EVE alone: 0.5 µM (A6); 0.25 µM (B6); 0.125 µM (C6), 0.06 µM (D6). EVE 0.5 µM (A-D2) with CP 10 µM (A2); CP 5 µM (B2), CP 2.5 µM (C2); CP 1.25 µM (D2). EVE 0.25 µM (A-D3) with CP 10 µM (A3); CP 5 µM (B3), CP 2.5 µM (C3); CP 1.25 µM (D3). EVE 0.125 µM (A-D4) with CP 10 µM (A4); CP 5 µM (B4), CP 2.5 µM (C4); CP 1.25 µM (D4). EVE 0.06 µM (A-D5) with CP 10 µM (A5); CP 5 µM (B5), CP 2.5 µM (C5); CP 1.25 µM (D5).

Figure 3.

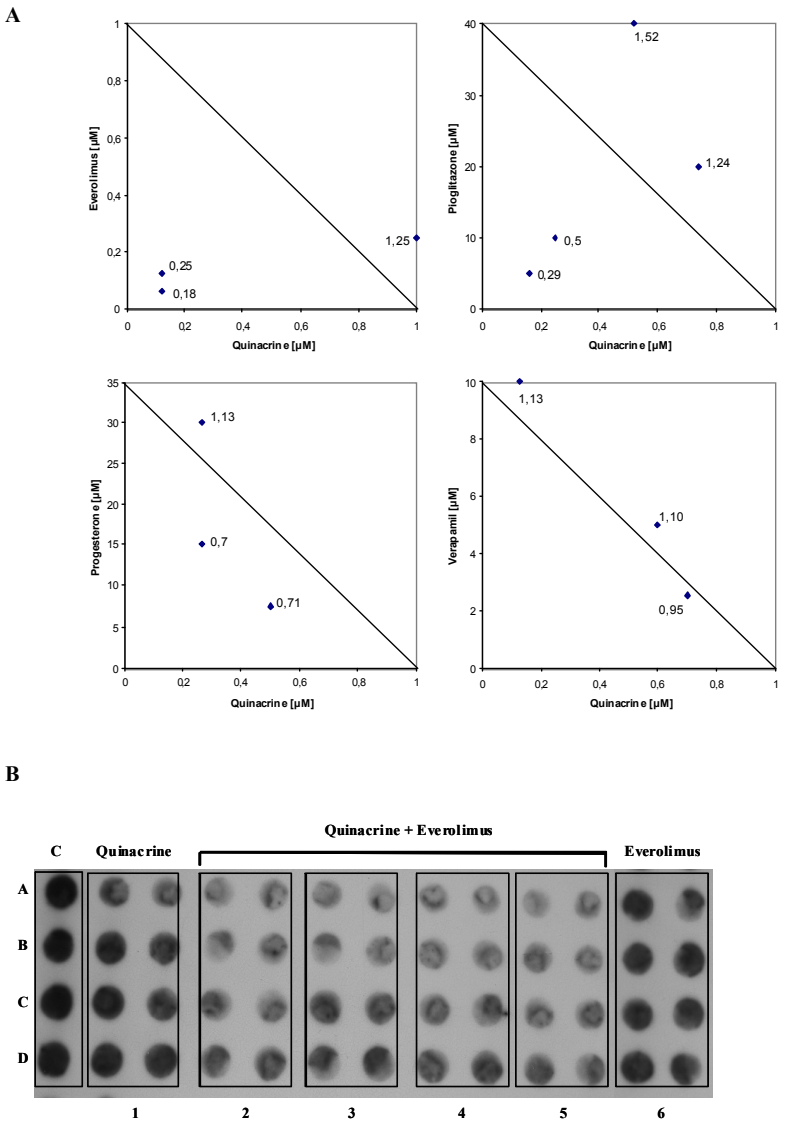

Figure 3. Anti-prion activity of quinacrine in combination with everolimus, pioglitazone, progesterone and verapamil. Prion-infected 22L-N2a cells were treated with different concentrations of everolimus, pioglitazone, progesterone and verapamil for 8 hours prior to the addition of different concentrations of quinacrine. After 96 hours, cells were lysed and processed for detection of PrP^{res} by dot blot with mouse monoclonal 6H4 (Prionics). A) Isoboles and FIC indices of combinations. B) A representative dot blot of the anti-prion effect of everolimus (EVE) and quinacrine (Q), alone and in combination. Controls (C A-D). Q alone: 1 µM (A1); 0.5 µM (B1); 0.25 µM (C1) and 0.12 µM (D1). EVE alone: 0.5 µM (A6); 0.25 µM (B6); 0.125 µM (C6), 0.06 µM (D6). EVE 0.5 µM (A-D2) with Q 1 µM (A2); Q 0.5 µM (B2), Q 0.25 µM (C2); Q 0.12 µM (D2). EVE 0.25 µM (A-D3) with Q 1 µM (A3); Q 0.5 µM (B3), Q 0.25 µM (C3); Q 0.12 µM (D3). EVE 0.125 µM (A-D4) with Q 1 µM (A4); Q 0.5 µM (B4), Q 0.25 µM (C4); Q 0.12 µM (D4). EVE 0.06 µM (A-D5) with Q 1 µM (A5); Q 0.5 µM (B5), Q 0.25 µM (C5); Q 0.12 µM (D5).

Figure 4.

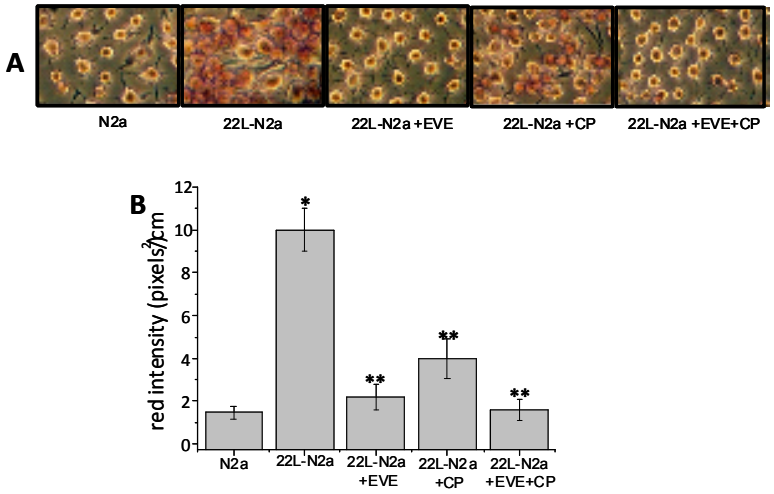

Figure 4. Oil red O staining of 22L-infected N2a cells after single and dual drug treatments. 22L-infected cells were incubated in the absence or in the presence of everolimus (EVE, 0.02μM) and chlorpromazine (CP, 2μM), alone or in combination. Control uninfected N2a cells were incubated in drug-free medium. After 96 hours, cell cultures were processed for evaluation of neutral lipid-bound oil red O. (A) Representative microscopic visualization of neutral lipid accumulation. (B) Quantitative measurements of oil red O staining. Data are expressed as mean pixel values /cm^2 of six created ROIs (Regions Of Interest) ±SE. *p<0.05, 22L-infected N2a cells vs. N2a cells; **p<0.05, treated vs. untreated 22L-infected N2a cells.

Figure 5.

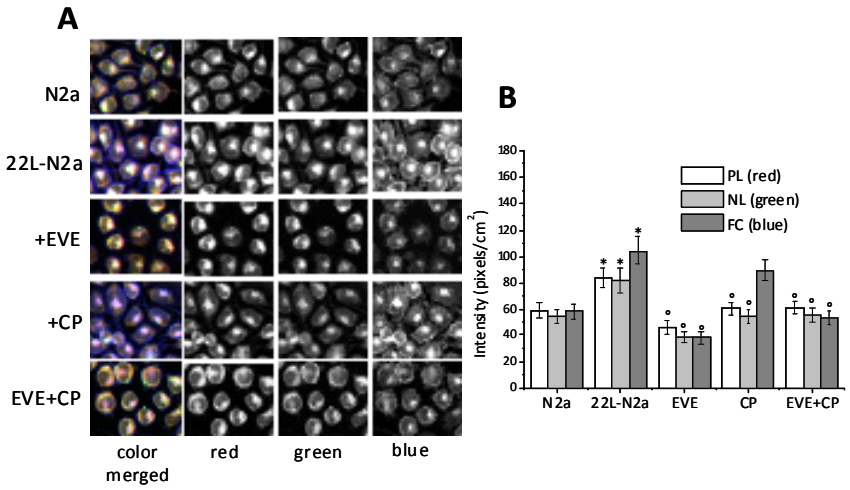

Figure 5. Nile red and filipin staining of 22L-infected N2a cells after single and dual drug treatments. 22L-infected cells were incubated in the absence or in the presence of everolimus (EVE, 0.02μM) and chlorpromazine (CP, 2μM), alone or in combination. Control uninfected N2a cells were incubated in drug-free medium. After 96 hours, cell cultures were stained with Nile red and filipin. (A) Representative microscopic visualization of stained cultures. NR-590 and NR-535 represent the red and green Nile red emissions which distinguish low-hydrophobic (i.e., phospholipids) and high-hydrophobic (i.e., triglycerides and cholesterol ester) lipids, respectively. Filipin stains free cholesterol. The three pictures are merged in the colour picture. Note that the white color, prevalent in 22L-infected cultures, is given by the overlay of the three signals. B) Quantitative analysis of Nile red and filipin staining. Data are the mean ± SD of the fluorescence intensity of NR-590, NR-535 and filipin staining. *p<0.05, 22L-infected N2a cells vs. N2a cells; °p<0.05, treated vs. untreated 22L-infected N2a cells.

Figure 6

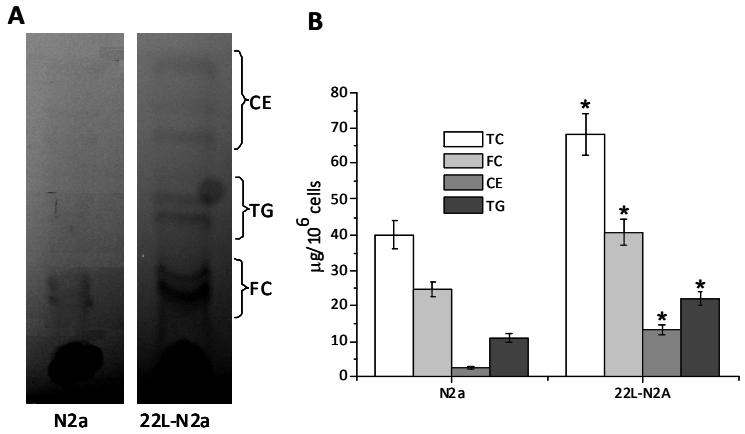

Figure 6. N2a vs. 22L-N2a lipid content by TLC. TL were extracted with cold acetone from triplicate N2a and 22L-N2a cell cultures. A total of $30x10^6$ of each cell culture was collected from sub-confluent flasks. Extracted lipids were split into two equal aliquots and air dried: one aliquot was used to determine TC by the cholesterol oxidase method; the other aliquot, after drying, was resuspended in 100 µl of chloroform and analysed for lipid subclasses by TLC on kiesegel plates as described in the Methods section. A) TLC separated bands as visualized by iodine vapor. B) TC, FC, CE and TG as determined by enzymatic methods. Data are the mean ± SE of triplicate cultures, *p<0.05, 22L-infected N2a cells vs. N2a cells; **p<0.05, treated vs. untreated 22L-infected N2a cells.

Figure 7

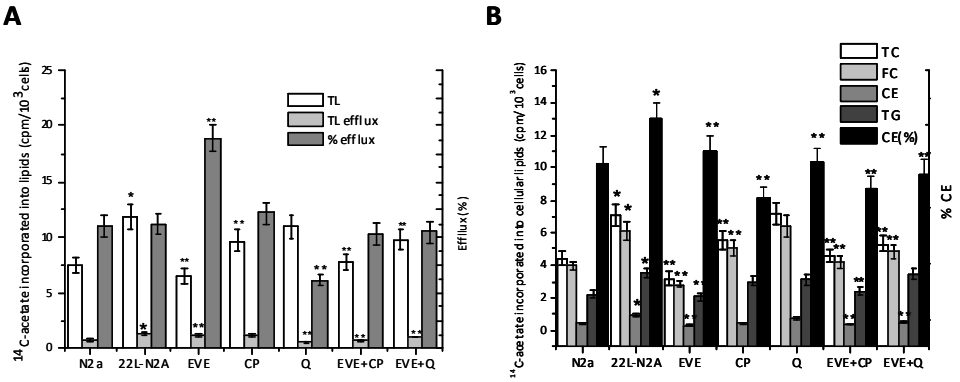

Figure 7. Effect of single vs. dual drug combinations on lipid synthesis and efflux. N2a and 22L-N2a cells were seeded at $1x10^4$/ml in flat-bottom 24-well plates. After overnight settlement, a set of 22L-N2a cultures were drug-treated (EVE, 0.02 µM; CP, 2 µM; Q, 0.2 µM) and further incubated for 72 hours. Cellular lipid syntheses (TC, FC, CE, TG) were evaluated by incubating cells for 6 hours in medium containing 2 µCi/ml of [1-^{14}C]acetate. After labeling, cells were washed with PBS and lipids extracted with cold acetone. Lipid subclasses were separated by thin layer chromatography (TLC) and [^{14}C]acetate incorporation into the various lipid fractions was measured. Efflux from the cells into the medium was expressed as the percentage of radioactivity in medium/total radioactivity (cells + medium). Each drug and drug combination was tested in triplicate. A) Total lipids and efflux; B) FC, CE, and TG. Data shown are the mean ± SE of triplicate cultures. *p<0.05, 22L-infected N2a cells vs. N2a cells; **p<0.05, treated vs. untreated 22L-infected N2a cells.